Lowering Carbon Emission with Autonomous Driving Vehicles

- Increasing Energy Savings with Advanced Power MOSFETs -

Martina Giuffrida [1)] Giusy Gambino [1)] Carmelo Mistretta [1)] Giuseppe Longo [1)] Filippo Scrimizzi [1)]

1) STMicroelectronics, Catania, Italy

E-mail: martina.giuffrida@st.com

E-mail: giusy.gambino@st.com

E-mail: carmelo.mistretta@st.com

E-mail: giuseppe-mos.longo@st.com

E-mail: filippo.scrimizzi@st.com

ABSTRACT: Today's industry players are accelerating the speed of automotive technology innovation as they develop new concepts of electric, connected, autonomous, and shared mobility. Major automotive megatrends for electrification and digitalization involve zone architectures, digital control of power devices, battery management systems, power / energy management and power electronics for autonomous driving. The advent of new smart integration strategies in Systems-in-Package (SIP) help improve fully autonomous vehicles' reliability with new high density and compact solutions, which enable increasing energy savings, thus improving the fuel efficiency of the vehicle and decreasing CO_2 emissions.

KEY WORDS: automotive megatrends, electrification, digitalization, autonomous driving, energy savings, CO_2 emission reduction.

1. INTRODUCTION

The trend of the worldwide market still reserves about 70% of the sales share for traditional ICE (Internal Combustion Engine) vehicles, while the remaining 30% includes overall xEV cars (all types of Hybrid and Electric Vehicles).

Technological trends in the automotive industry are boosting the production of self-driving cars, improving safety thanks to the reduction of human drivers on the road and use of advanced solutions, like computer vision and prediction systems of pedestrian behavior. Autonomous driving helps improve also vehicles' reliability with new high density and compact solutions and protection circuits with prompt interventions to prevent any damage to the vehicle itself and passengers. Advanced Driver Assistance Systems (ADAS) are able to bring benefits to power efficiency and then greenhouse gas emissions, travel times and road congestion.

Energy savings play a key role in the development of new smart integration strategies implemented with System-in-Package (SIP) solutions which show the following advantages:

- smart use of different technologies in a system integrating both complex power and signal circuits;
- extremely compact system housed in a tiny automotive package;
- attractive performance in terms of faster switching, higher power efficiency and lower electromagnetic interference (EMI);
- affordable cost for the optimized system blocks and reduced bill of material (BOM) for filtering.

Autonomous driving applications require buck, boost or buck-boost converters to power both the main CPU and memory slots with integrated temperature and current sensing protection circuits. [(1)]

Advanced power MOSFETs with optimized figure of merit in terms of both conduction and switching performance can be used to supply and stabilize voltage and current levels with a fast dynamic loading variation, to satisfy the stringent specifications of the automotive standards. [(2, 3)]

From technology point of view, the new wide-bandgap devices, such as GaN FETs, are capable of very high performance, allowing SiP power conversion system to obtain high switching frequencies and good thermal behavior at temperatures over 200 °C.

However, for Low Voltage (LV) application, pure Silicon (Si) MOSFETs are very competitive in terms of conductions losses compared with LV GaN FETs available in the market. Then, the relevant SiP system is very competitive achieving both low-cost and high-performance. [(4)]

2. INTEGRATED MOSFET – BASED SYNCHRONOUS CONVERTER

A synchronous DC-DC converter with a MOSFET–based power stage is integrated into a SiP with integrated temperature and current sensing circuits as well as gate driver circuits. (5)

The simplified block diagram of the SiP is shown in Fig. 1.

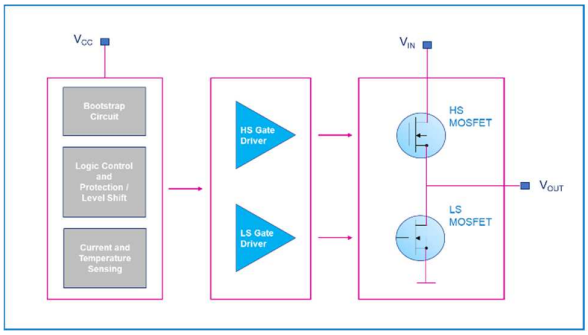

Fig. 1 Schematic block diagram of the system in package.

To match the stringent requirements of autonomous driving systems, a multiphase synchronous buck is considered, using 3 or 4 SiP's, which are capable of delivering up to 50 A each at a nominal switching frequency of 600 kHz. Additional protection features are considered to detect short circuit, over current and overvoltage issues with the possibility of preventing any faults thanks to a real-time diagnostic performed through a high accurate temperature and current sensing. This type of device is commonly referred to as DrMOS as it includes both the controller/driver chip and half bridge power stage in a single small package.

For autonomous driving applications, the interleaved configuration for the buck and boost converter is the most viable solution as it strongly improves the current output waveforms quality reducing the ripple. Furthermore, the size of the output filter decreases in an interleaved implementation due to the lowered current in the power switching leg for each phase. The number of the operating switching legs can be activated according to the load request optimizing the device current share. (6)

Selecting the maximum number of the switching legs (generally 4 for feeding the main CPU and 2 for the memory slot), the current in the single device is reduced, acting in the power MOSFET heating reduction. (7)

A simplified block diagram of the power supply based on the SiP MOSFET half-bridge converter in interleaved configuration, implementing 3 switching legs is reported in Fig. 2.

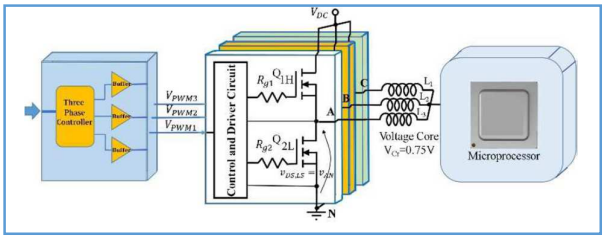

Fig. 2 Block diagram of power supply with SiP converter.

The power MOSFETs of the DC-DC converter play a key role for the carbon emission reduction as they strongly affect the power conversion performance and therefore the behavior of the overall system.

The STPOWER STripFET F8 MOSFETs are fully AEC-Q101 qualified to meet the requirements of harsh automotive environments. They have an optimized design to improve the figure of merit, by reducing both the static on-resistance and dynamic parameters, such as the reverse transfer capacitance and gate-drain charge. Thanks to this, the STripFET F8 MOSFETs ensure switching speeds at frequencies up to 2 MHz.

3. EXPERIMENTAL DATA

An asymmetric half-bridge converter with STripFET F8 power low side (LS) and high side (HS) MOSFETs has been experimentally analyzed with gate protection and sensing circuits.

The operative conditions of the proposed devices for the power supply have been extended from 600 kHz to 2 MHz.

3.1. Main Parameters

The main electrical parameters of the SiP are reported in Table 1.

Table 1 Main electrical parameters of the SiP.

Symbol	Parameter	Value	Unit
VIN	Input voltage	12	V
VOUT	Output voltage	1.0-1.1	V
IOUT	Output current	50 (max value)	A
DT	Duty cycle	10 (variable to keep VOUT = 1 V)	%
fsw	Switching frequency	600 - 2000	kHz
LOUT	Output inductance	0.15	µH

The main electrical parameters of the LS and HS STripFET F8 MOSFETs are reported in Tables 2 and 3.

Table 2 Main electrical parameters of the HS MOSFET.

Symbol	Parameter	Value	Unit
RDSon	Static drain-source on-resistance	4 @ 25°C 6 @ 100°C	mΩ
Qg	Total gate charge	11 (max value)	nC

Table 3 Main electrical parameters of the LS MOSFET.

Symbol	Parameter	Value	Unit
RDSon	Static drain-source on-resistance	1.2 @ 25°C 1.8 @ 100°C	mΩ
Qg	Total gate charge	29.4 (max value)	nC

It is worth considering that the HS MOSFET shows very low gate charge to reduce the switching losses and the LS switch very low static on-resistance to reduce the conduction losses.

3.2. Measured Results for the SiP

The overall efficiency of the system has been measured at 3 different frequencies (600kHz, 1.2MHz and 2MHz), as shown in Fig. 3.

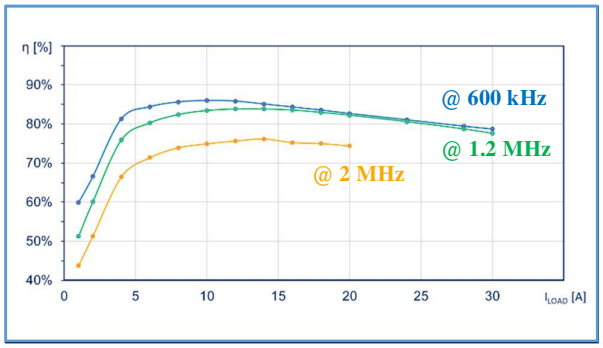

Fig. 3 Measured efficiency of the system at different frequencies.

Experimental data shows that power efficiency achieves values in the range of 80% for currents up to 30A and frequencies above 1 MHz.

The real-time telemetry is accomplished through temperature and current sensing and the following graphs (Figs. 4 and 5) show the comparison between detected and measured data.

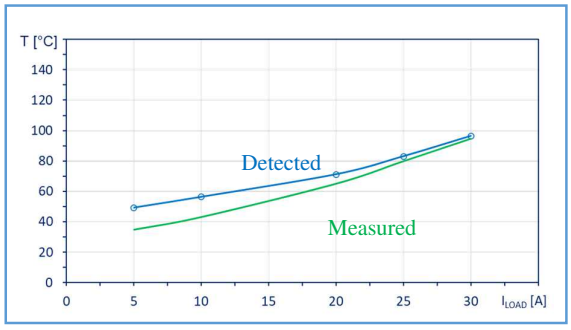

Fig. 4 Temperature sensing @ 600 kHz.

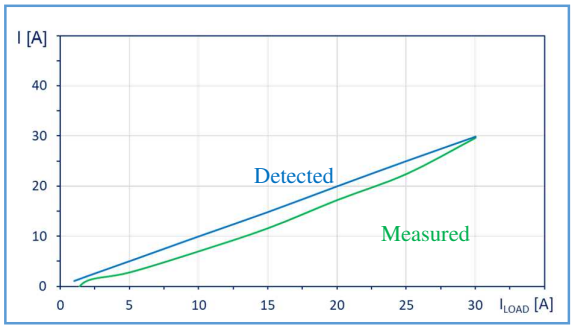

Fig. 5 Current sensing @ 600 kHz.

In both cases, experimental data shows that real-time telemetry provides high accuracy for a wide range of the load current.

Protection circuits have been designed to stop the SiP operation when an anomalous condition is detected. The following graph (Fig. 6) shows how the under-voltage protection works when the supply voltage of the LS gate driver (V_{DRIVER}) drops below 4V.

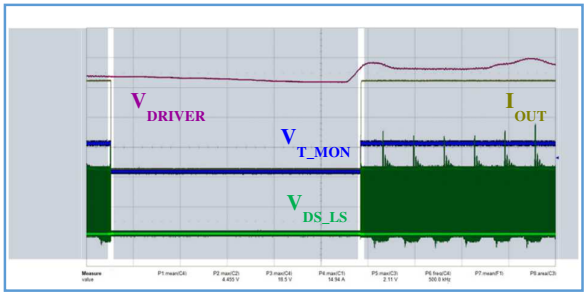

Fig. 6 Driver under-voltage protection @ 600 kHz.

In this case the controller pulls down the flag signal (V_{T_MON}), thus inhibiting the system operation (the switch node voltage equal to V_{DS_LS} – green trace – drops down to 0 V) and then the output current (I_{OUT}) delivery.

Once the fault event is removed, the V_{T_MON} voltage goes back to high level and the system restarts the normal operations.

In the event of an over-temperature condition, the output voltage of the temperature sensor (V_{T_sense}) exceeds the over-temperature

threshold (3.3 V) and, therefore, the protection circuit inhibits the system operation (Fig. 7).

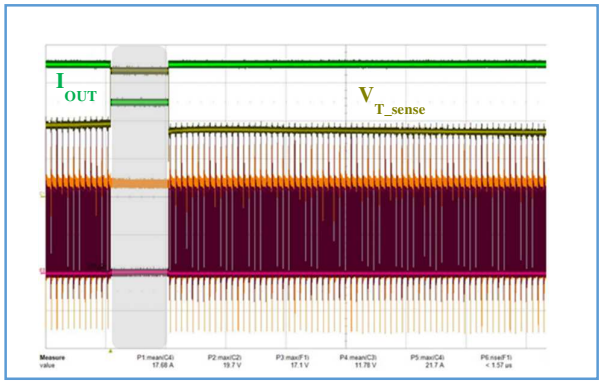

Fig. 7 Over-temperature protection @ 600 kHz.

In this case, the switch node voltage (V_{DS_LS} – purple trace) drops to 0 V and the output current (I_{OUT}) is no longer supplied.

Once the fault event is removed, the V_{T_sense} voltage goes back to the nominal value and the system restarts the normal operations, as shown by the detailed measured waveforms in Fig. 8.

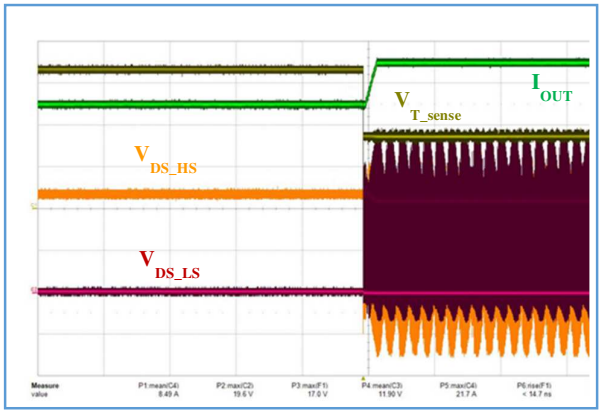

Fig. 8 Detailed measured waveforms relevant to the over-temperature protection @ 600 kHz.

All the added features of the SiP, in terms of current and temperature sensing as well as under-voltage and over-temperature protections, enable real-time telemetry for diagnostics and prevention on CPU and memory slot usage. This ensures a high level of accuracy and flexibility which maximize the reliability and safety of the entire system.

3.3. Measured Results for the DC-DC Converter

The experimental data for the STripFET F8 MOSFETs are relevant to the following conditions:

- V_{IN} = 12 V
- I_{LOAD} = 20 A
- f_{sw} = 600 kHz

which are the typical values of the input voltage, load current and switching frequency, respectively.

The measured waveforms for the LS and HS MOSFETs in steady conditions with a zoomed view of the switching transients are shown in Fig. 9 (a and b).

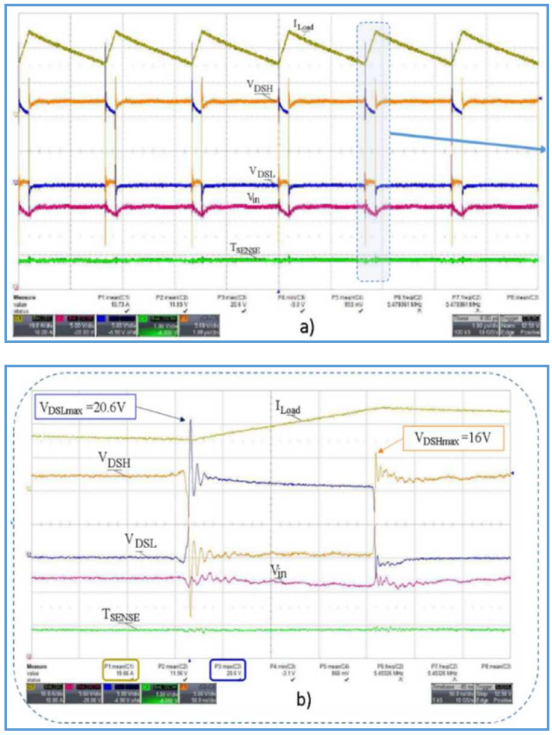

Fig. 9 Measured waveforms for LS and HS MOSFETs (a) and zoomed switching transients (b) @ 600 kHz.

The load current waveform can be improved by using an interleaved configuration able to reduce the ripple through the activation of the operating switching legs to meet the load request. This improves the current sharing among the different legs and then optimizes the thermal performance and power efficiency with high load currents.

The measured waveforms relevant to 2 switching legs in interleaved configuration with a zoomed view of the switching transients are shown in Fig. 10 (a and b).

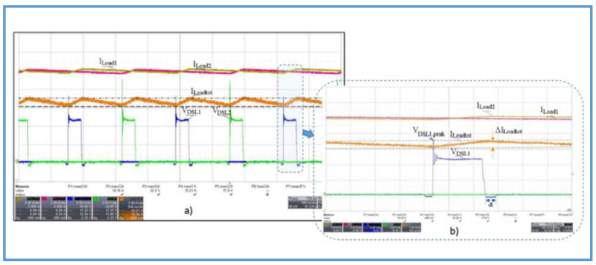

Fig. 10 Measured waveforms in interleaved configuration (a) and zoomed switching transients (b) @ 600 kHz.

The experimental data show that the interleaved configuration improves both the voltage and current ripple. In fact, the maximum peak on the LS voltage is lowered to 17.8 V and the ripple peak of the load current is 0.5 A. Then, the DC-DC converter is able to supply and stabilize the output voltage and current at safe values.

4. CONCLUSION

The measured behavior of the SiP has been shown with both single-phase and interleaved working conditions. The sensing and protection features have been experimentally analyzed, showing their impact on the overall performance of the system.

Finally, the benefits of the STPOWER STripFET F8 technology have been demonstrated with AEC Q101 power MOSFETs capable of operating at high frequencies with high levels of efficiency.

Thanks to the energy savings optimization, the proposed SiP solution makes a significant contribution to boost the vehicle efficiency, thus lowering carbon emissions while maintaining fast matching to dynamic load variation and stability in current and voltage setting.

REFERENCES

(1) J. A. Baxter, D. A. Merced, D. J. Costinett, L. M. Tolbert and B. Ozpineci, “Review of Electrical Architectures and Power Requirements for Automated Vehicles,” *2018 IEEE Transportation Electrification Conference and Expo (ITEC)*, pp. 944-949, Long Beach, CA, USA, 2018.

(2) S. Musumeci, R. Pagano, A. Raciti, G. Belverde, M. Melito, “Low–voltage MOSFETs with improved performances in advanced DC-DC converter applications,” *Proceedings of the EPE 2003 Conference*, pp. 1-10, Toulouse, France, 2-4 Sept. 2003.

(3) N. Mohan, T. M. Undeland, W. P. Robbins, *Power electronics converters, applications and design*, 2nd ed. Wiley & Sons NY, 1995.

(4) E. Armando, S. Musumeci, F. Fusillo, F. Scrimizzi, “Low voltage trench-gate MOSFET power losses optimization in synchronous buck converter applications,” *21st European Conference on Power Electronics and Applications*, Sept. 2019.

(5) C. O'Mathuna, "PwrSiP power supply in package power system in package," *2016 International Symposium on 3D Power Electronics Integration and Manufacturing (3D-PEIM)*, pp. 1-21, Raleigh, NC, USA, 13-15 June 2016.

(6) X. Yang, S. Zong and G. Fan, "Analysis and validation of the output current ripple in interleaved buck converter," *43rd Annual Conference of the IEEE Industrial Electronics Society (IECON)*, pp. 846-851, Beijing, China, 29 Oct.-1 Nov. 2017.

(7) B. Murari, F. Bertotti, G. Vignola, "Smart Power ICs", *2nd Edition, Springer Verlag*, Berlin, 2002.